

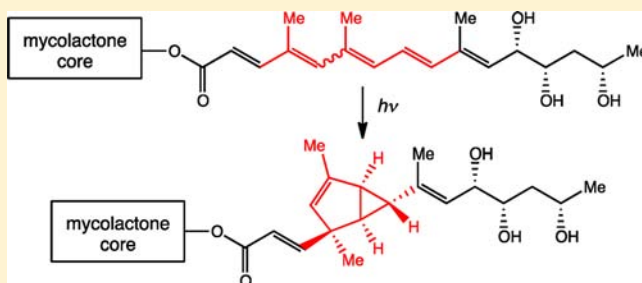
# Photochemistry of Mycolactone A/B, the Causative Toxin of Buruli Ulcer

Yalan Xing,<sup>†</sup> Sudhir M. Hande,<sup>†</sup> and Yoshito Kishi\*

Department of Chemistry and Chemical Biology, Harvard University, Cambridge, Massachusetts 02138, United States

**S** Supporting Information

**ABSTRACT:** Photochemistry of mycolactone A/B and related unsaturated fatty acid esters is reported. On exposure to visible light, mycolactone A/B gave a mixture of four photomycolactones. Pentaenoates and tetraenoates, representing the unsaturated fatty acid portion of mycolactone A/B, were found to show the reactivity profile parallel with that of mycolactone A/B. The structure of the four photomycolactones was elucidated via (1) structure determination of the four photoproducts in the tetraenoate series; (2) their transformation to the photoproducts in the pentaenoate and then mycolactone series. Triplet quenchers did not affect the photochemical transformation, thereby indicating an event at the singlet state. A concerted, photochemically allowed  $[4\pi s + 2\pi a]$  cycloaddition was suggested to account for the observed result. This study provided the structurally defined and homogeneous material, which allowed demonstration that photomycolactones exhibit significantly reduced cytotoxicity, compared with mycolactone A/B.



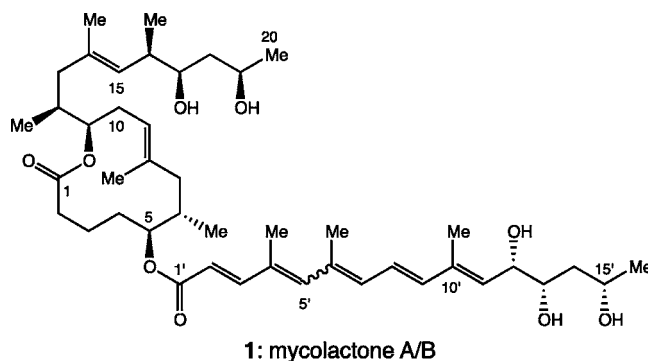
## INTRODUCTION

**Background.** Buruli ulcer is a severe and devastating skin disease caused by *Mycobacterium ulcerans* infection, yet it is one of the most neglected diseases.<sup>1</sup> Infection with *M. ulcerans* results in progressive necrotic lesions that, if untreated, can extend to 15% of a patient's skin surface. Surgical excision/skin grafting was the only method for treatment of Buruli ulcer. Encouragingly, it has recently been reported that most patients respond to combination treatments with rifampin and streptomycin.<sup>2</sup>

In 1999, Small and co-workers isolated and characterized two polyketide-derived macrolides, named mycolactones A and B, from *M. ulcerans* 1615.<sup>3</sup> Mycolactones A and B were shown to exhibit cytotoxic and immunosuppressive activities and also to reproduce the natural pathology of Buruli ulcer on a guinea pig model.<sup>4</sup> The gross structure of mycolactones A and B was elucidated with spectroscopic methods, whereas the stereochemistry was predicted via the universal NMR database approach and confirmed by total synthesis.<sup>5–8</sup> Under standard laboratory conditions, mycolactones A and B exist as a rapidly equilibrating 3:2 mixture of  $\Delta^{4',5'}\text{-Z}$  (major) and  $\Delta^{4',5'}\text{-E}$  (minor) isomers, and are referred to as mycolactone A/B in this contribution (Scheme 1).

Because of the slow-growing and pathogenic nature of *M. ulcerans*, it was a challenging task to secure mycolactones in quantity by cultivation. With the development of convergent, scalable, and flexible syntheses, we now have access to the mycolactone as a structurally defined material in quantity. We have been interested in the chemical and biological properties of mycolactones and initiated the study on their chemical

## Scheme 1. Structure of Mycolactone A/B<sup>a</sup>



<sup>a</sup>Mycolactone A/B exists as a rapidly equilibrating 3:2 mixture of  $\Delta^{4',5'}\text{-Z}$  (major) and  $\Delta^{4',5'}\text{-E}$  (minor) geometric isomers under standard laboratory conditions.

stability. Coincident with this activity, we learned from Professor Britton, Karolinska University Hospital, Stockholm, Sweden, that natural mycolactone A/B, on exposure to light for 30 min, completely loses its toxicity against keratinocytes.<sup>9</sup> A literature search revealed an interesting history on light-irradiation of mycobacteria, including *M. ulcerans*, for potential medical applications.<sup>10</sup>

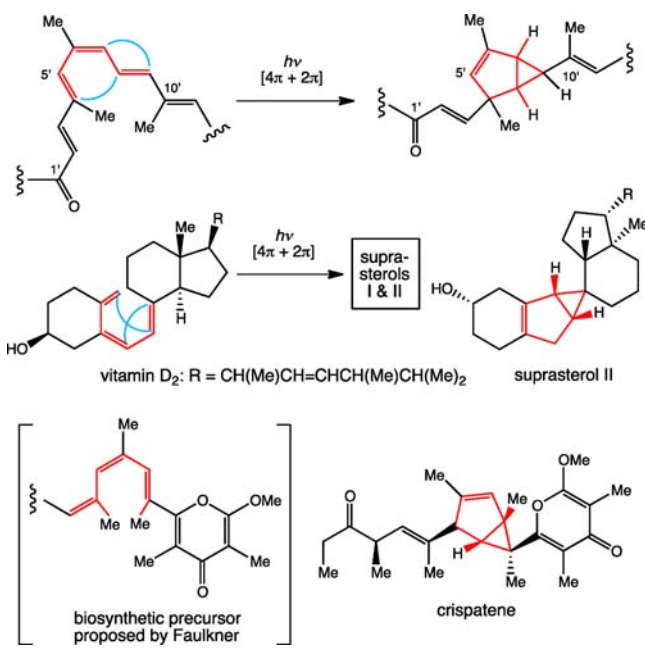
Received: September 17, 2012

Published: November 2, 2012

## RESULTS AND DISCUSSION

**Photochemistry of Mycolactone A/B.** With this background, we began the photochemical study of synthetic mycolactone A/B (UV (MeOH)  $\lambda_{\max}$  362 nm ( $\log \epsilon$  4.35)). On exposure to light through a 365 nm filter in acetone at rt, we observed a clean transformation of mycolactone A/B to “photomycolactone”. Spectroscopic studies (MS and  $^1\text{H}$  NMR) proved the following: (1) “photomycolactone” consists of four closely related compounds, (2) all of them are isomers of mycolactone A/B, and (3) all of them have the C2'–C3' and C10'–C11' olefins intact. On the basis of these data, we speculated that the photochemically induced isomerization was due to a  $[4\pi + 2\pi]$  cycloaddition on the central triene moiety (Scheme 2). The photochemically induced transformation of

**Scheme 2. Possible Pathway for Photochemically Induced  $[4\pi + 2\pi]$  Cycloaddition and Relevant Examples**

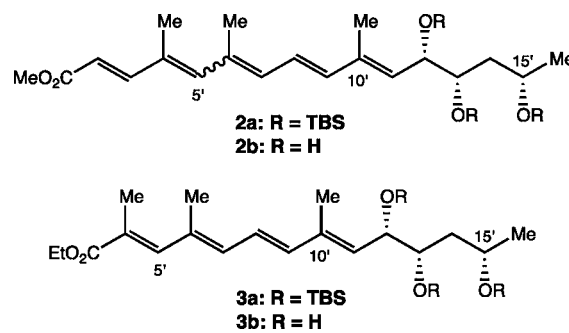


vitamin D  $\rightarrow$  suprasterols is a historical example for this class of reactions (Scheme 2).<sup>11,12</sup> There are some natural products known to contain the bicyclo[3,1,0]hexene structure, including crispatene reported by Scheuer and then by Faulkner.<sup>13,14</sup> Faulkner proposed the triene as the possible biosynthetic precursor and suggested a photochemical  $6\pi$  conrotatory and  $[\sigma 2a + \pi 2a]$  electrocyclizations for the biosynthetic pathway. Notably, Faulkner isolated the 1,3-cyclohexadiene-containing natural product as a co-occurring metabolite and demonstrated its photochemical transformation into the bicyclo[3,1,0]hexene structure.

In order to facilitate the stereochemistry assignment, we attempted to separate the four photomycolactones, but with only limited success. Under these circumstances, we examined the photochemical behavior of several different substrates, including TBS-protected and nonprotected methyl pentaenoates **2a,b** and TBS-protected and nonprotected ethyl tetraenoates **3a,b** (Scheme 3).<sup>15</sup>

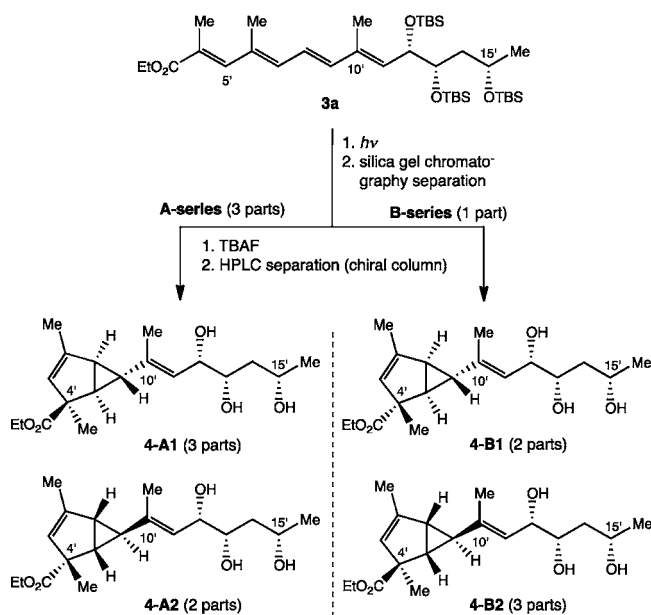
**Photochemistry of Unsaturated Fatty Acid Esters.** On exposure to light through a 365 nm filter or sunlight, all of the substrates exhibited a very similar reactivity, namely a rapid  $E \rightleftharpoons Z$  isomerization of olefinic bonds, followed by cyclization, to

**Scheme 3. Four Unsaturated Fatty Acid Esters Studied**



yield a mixture of four products. With silica gel chromatography, the four products were first separated into A- and B-subgroups.<sup>16</sup> However, it was challenging to separate two compounds present in each subgroup. After many attempts, we were able to achieve the separation of the four photoproducts in the tetraenoate series as summarized in Scheme 4.

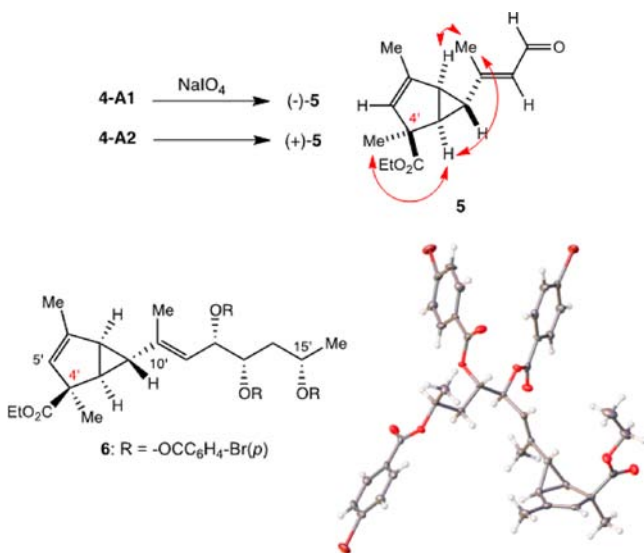
**Scheme 4. Separation and Structure of the Four Stereoisomers Obtained in the Photochemistry of Tetraenoate 3a<sup>a</sup>**



<sup>a</sup>Note that the major and minor products in the B-series are tentatively assigned as **4-B2** and **4-B1**, respectively.

**Stereochemistry of the Four Photoproducts in the Tetraenoate Series.** With the four separated stereoisomers in hand, we were able to address their stereochemistry. In the A-series, periodate oxidation of **4-A1** and **4-A2** yielded the same aldehyde **5**, but in levorotatory and dextrorotatory forms, respectively. This experiment established **4-A1** and **4-A2** to be remote diastereomers where the absolute configuration differed at each of the stereogenic centers in the C4'–C9' portion of the structure, while being the same in the C12'–C15' subunit (Scheme 5).<sup>17</sup> The relative stereochemistry of **5** was deduced from NOE experiments, cf. double-headed arrows to show the proton-connectivity relevant to this assignment. We attempted a few methods to establish its absolute stereochemistry, but were unable to secure the definitive evidence. Meanwhile, we

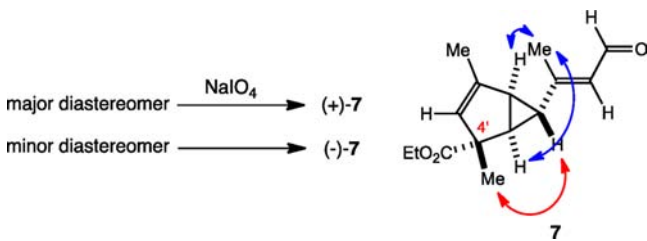
## Scheme 5. Stereochemistry Assignment of 4-A1 and 4-A2



were able to obtain the tri-*p*-bromobenzoate of 4-A1 in a crystalline form, the X-ray analysis of which established the structure of 4-A1, and consequently 4-A2, as shown in Schemes 4 and 5.

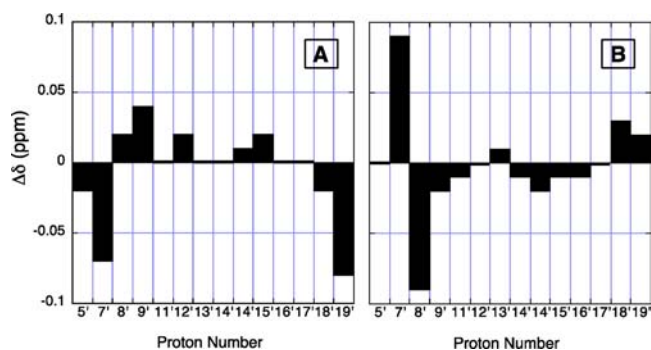
Similarly, the major and minor diastereomers in the B-series were subjected to periodate-oxidation, to give aldehyde 7 in dextrorotatory and levorotatory forms, respectively. Once again, NOE experiments established the relative stereochemistry of 7, thereby showing that aldehyde 7 was the C4' diastereomer of aldehyde 5. This experiment demonstrated that the major remote diastereomer corresponds to either 4-B1 or 4-B2, and the minor to the other (Scheme 6).

## Scheme 6. Relative Stereochemistry of Aldehyde 7 Derived from the Major and Minor Diastereomers in the B-series



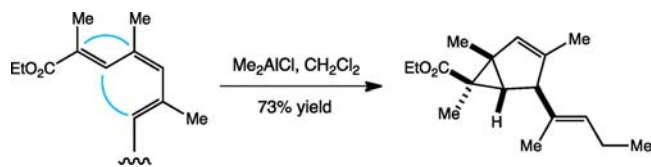
In spite of considerable efforts, we were unable to secure a crystal suitable for an X-ray analysis in the B-series. Thus, we relied on the spectroscopic method and examined the  $^1\text{H}$  and  $^{13}\text{C}$  chemical shift differences, i.e.,  $\Delta\delta = \delta_{\text{A major}} - \delta_{\text{A minor}}$  vs  $\Delta\delta = \delta_{\text{B major}} - \delta_{\text{B minor}}$ . For illustration, Figure 1 shows the  $^1\text{H}$   $\Delta\delta$  between the A- and B-series.<sup>18</sup> Our interest was to deduce the relative stereochemistry between the pre-existing C12'–C15' subunit and the newly formed bicyclo[3,1,0]hexene moiety. Interestingly, the C7'-, C8'-, and C9'-protons in Panel B of Figure 1 exhibited the  $\Delta\delta$  in the opposite sign of those in Panel A, thereby suggesting that 4-A1 and 4-B2, and 4-A2 and 4-B1, share the same relative stereochemistry with respect to these two subunits. Thus, we tentatively assigned the major and minor diastereomers as 4-B2 and 4-B1, respectively.

Related to the reported photochemically induced  $[4\pi + 2\pi]$  cycloaddition, we quote the stereoselective, Lewis acid-promoted  $[4\pi + 2\pi]$  cyclization reported by Trauner (Scheme



**Figure 1.** Difference in proton chemical shifts between the TBS-protected major and minor products in the A- and B-series, respectively. (Panel A)  $\Delta\delta$  ( $\delta_{\text{A major}} - \delta_{\text{A minor}}$ ). (Panel B)  $\Delta\delta$  ( $\delta_{\text{B major}} - \delta_{\text{B minor}}$ ).

7).<sup>19</sup> For this case, the  $4\pi$ - and  $2\pi$ -components are inverse to those in the photochemical cycloaddition.

Scheme 7. Lewis Acid-Promoted  $[4\pi + 2\pi]$  Cycloaddition Reported by Trauner

**Mechanistic Considerations.** The transformation reported appeared to involve a photochemically induced  $[4\pi + 2\pi]$  cycloaddition. Unlike pentaenoates and mycolactone A/B, we anticipated that tetraenoates would be stable under the standard laboratory conditions and, therefore, are better suited for studying the process.<sup>20</sup> On exposure to light through a 365 nm filter for 2.5 h at 30 °C in acetone, tetraenoate 3a gave an approximately 2:7:1:1 mixture of geometrical isomers free from the cyclization products.<sup>21</sup> As hoped, these products were stable and separable with HPLC. Spectroscopic studies, including NOESY NMR experiments, allowed us to conclude 4'E,6'E,8'E,10'E (2 parts), 4'Z,6'E,8'E,10'E (7 parts), 4'E,6'Z,8'E,10'E (1 part), and 4'Z,6'Z,8'E,10'E (1 part), respectively.<sup>15</sup> An accumulation of 4'E,6'Z,8'E,10'E and 4'Z,6'Z,8'E,10'E tetraenoates indicated the rate-limiting step of transformation to be the  $[4\pi + 2\pi]$  cycloaddition, rather than the  $E \rightleftharpoons Z$  isomerization to form 6'Z-olefins required for the cycloaddition. The 2:7:1:1 ratio of geometrical isomers appeared to represent the ratio at the photochemical steady state, as an approximately same ratio was observed at the 40% and 70% completion of cycloaddition. The A- and B-subgroup products were derived from the 4'E,6'Z- and 4'Z,6'Z-isomers, respectively, and the 3:1 ratio of two-subgroup products seemed to reflect the relative cycloaddition-rate from the 4'E,6'Z- and 4'Z,6'Z-isomers to each cyclization product.

We note an interesting, additional observation. Due to the stereogenic centers at the C12'–C15' moiety, we expected to observe a 1:1 mixture of two remote diastereomers, because the photocyclization site was remote from the pre-existing stereogenic centers. However, the experimental results showed that the remote stereogenic centers affected the direction of the tetraenoates coiling in the photocyclization process.<sup>22</sup>

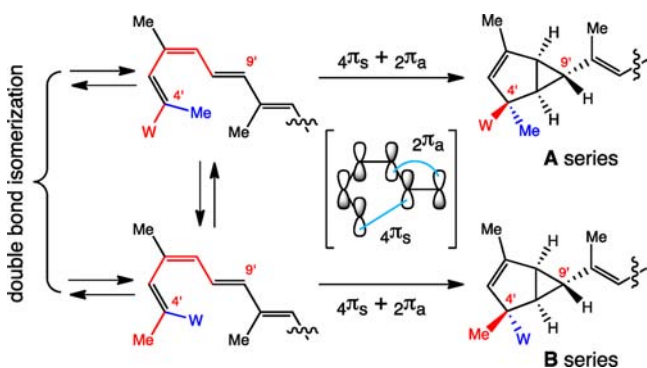
Intriguingly, this photochemistry showed a temperature dependency; the transformation was completed in 105, 48,

33, 35 h at 10, 20, 30, and 40 °C, respectively. We would attribute the observed temperature dependency to the specific coiled-conformation required for the tetraenoates to enter into the  $[4\pi + 2\pi]$  cycloaddition.<sup>23</sup>

The transformation proceeded well in acetone, tetrahydrofuran, ethyl acetate, and acetonitrile, but not in methylene chloride, chloroform, and benzene. In addition, the transformation took place smoothly in methanol and aq glyme (glyme:H<sub>2</sub>O = 5:1), to give the four photoproducts, with the improved A-/B-subgroup selectivity (6:1 in methanol and 10:1 in aq glyme), but did not affect remote diastereomer selectivity between the C4'-C9' and C12'-C15' subunits (3:2).

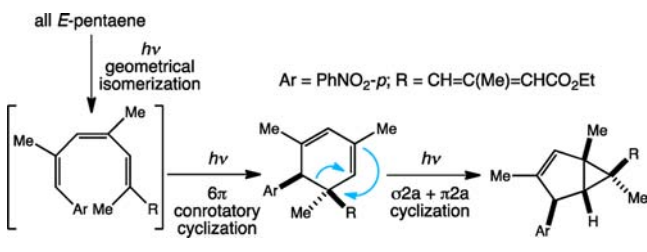
The photochemistry of **3a** was not affected by triplet quenchers such as azulene, ferrocene, and rubrene in tetrahydrofuran and acetonitrile. On the other hand, the photochemistry in the presence of a triplet sensitizer benzophenone in acetonitrile gave only unidentified products but no photoproducts **4-A,B**. These results indicate that this photochemically induced transformation took place at the singlet state.<sup>24</sup> Coupled with its stereospecificity, we suggest a concerted  $[4\pi_s + 2\pi_a]$  cycloaddition for the cyclization (Scheme 8).

Scheme 8. Proposed  $[4\pi_s + 2\pi_a]$  Cycloaddition



Related to the proposed  $[4\pi_s + 2\pi_a]$  cycloaddition, we comment on the work by Baldwin and co-workers (Scheme 9).<sup>25</sup> For the biosynthesis of photodeoxytridachone, they

Scheme 9. Two-Step Photochemical Rearrangements Reported by Baldwin

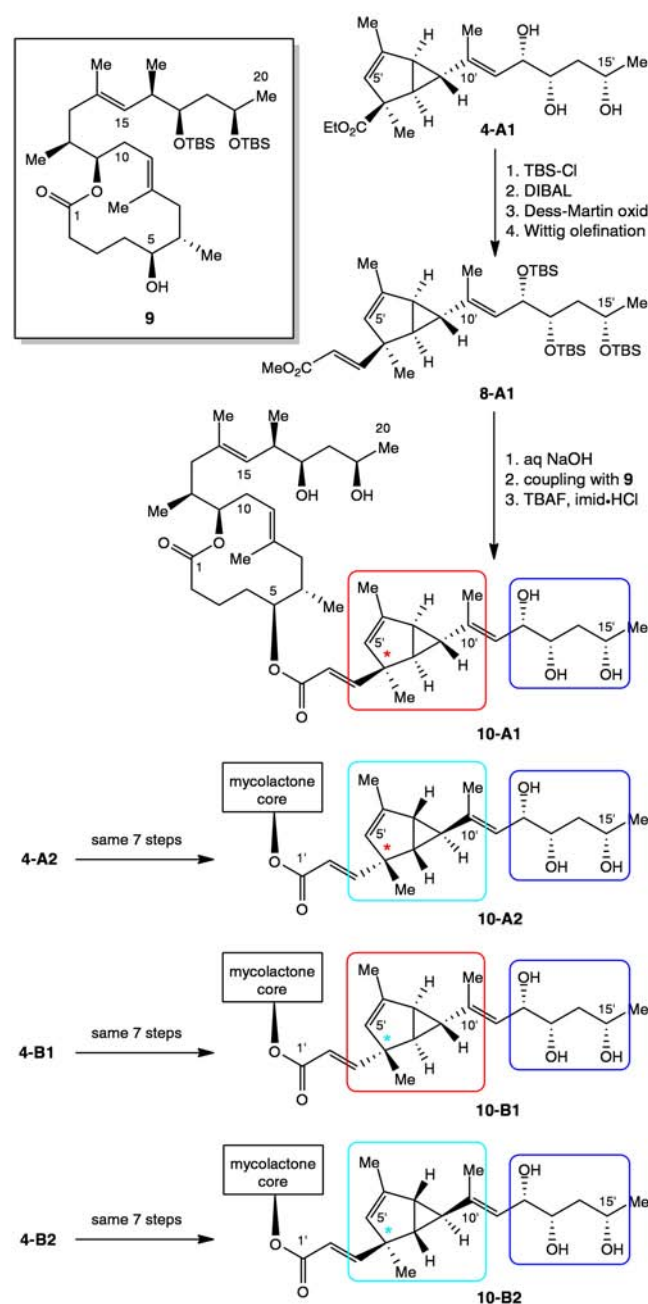


suggested all-*trans*-polyene as the biosynthetic precursor, which is transformed into the bicyclo[3,1,0]hexene structure via photochemically induced double-bond isomerization,  $6\pi$  conrotatory cyclization, and  $[\sigma_2a + \pi_2a]$  cyclization. Notably, they isolated the 1,3-cyclohexadiene intermediate and demonstrated that it was quantitatively converted to the bicyclo[3,1,0]hexene under photochemical conditions. For two reasons, however, we believe it to be unlikely that the photochemical transformation reported here follows this

pathway. First, despite the product analysis at early and late stages of photochemistry, we did not detect the 1,3-cyclohexadiene in a reaction mixture (<sup>1</sup>H NMR). Second, we used a 365 nm filter (cutoff wavelength: ~340 nm) for the photochemistry so that the 1,3-cyclohexadiene chromophore is unlikely excited.

**Transformation of the Tetraenoate Photoproducts into the Pentaenoate and then Mycolactone Photoproducts.** In order to correlate the photoproducts in the tetraenoate series with those in the pentaenoate and mycolactone series, we carried out the transformations outlined in Scheme 10. The efficiency of the synthetic sequence was excellent, and the final products, as well as the synthetic intermediates, were isolated and fully characterized. Impor-

Scheme 10. Correlation of the Tetraenoate Series with the Pentaenoate and Mycolactone Series



tantly, this experiment not only furnished structurally defined and homogeneous photomycolactones but also provided us with the opportunity of demonstrating that the product distribution in the tetraenoate series nicely matched that in the pentaenoate as well as mycolactone series, including the ratio of A-/B-subgroup products and remote diastereomers.

The availability of structurally defined materials allowed us to search for unique characteristics to differentiate the photomycolactones from mycolactone A/B and also from each other. Indeed, it was rather straightforward to differentiate them by  $^1\text{H}$  NMR chemical shifts and HPLC retention times.<sup>15</sup>

However, we should note that mycolactone A/B and photomycolactones were indistinguishable in MS spectroscopy, including MS/MS spectra, thereby presenting a challenge to monitor the photochemical isomerization in a living system.<sup>26</sup> Also, because of the lack of pentaenoate chromophore, the HPLC detection sensitivity of photomycolactones is not as high as that of mycolactone A/B, thereby posing the same challenge.<sup>27</sup>

The availability of structurally defined and homogeneous photomycolactones also allowed us to study their biological properties. As noted in the introduction, natural mycolactone A/B was reported to exhibit cytotoxic and immunosuppressive activities. Thus far, we have studied the cytotoxicity against five cell lines, thereby demonstrating that all four of the photomycolactones exhibit significantly reduced toxicity.<sup>28</sup> This result hints at the possibility of detoxifying mycolactones with visible light irradiation. In the opposite direction, it suggests a possible structure modification, for example, reduction of the C6'-C7' double bond, to avoid the photocycloaddition and maintain the cytotoxicity of mycolactones.

Lastly, we comment on a recent work that reported the photodegradation of natural mycolactone A/B.<sup>29</sup> Notably, the disclosed spectroscopic data (MS,  $^1\text{H}$  NMR) indicate that none of the photomycolactones from the current study corresponds to the photodegradation product reported.

## CONCLUSION

We reported the photochemistry of mycolactone A/B and related unsaturated fatty acid esters. On exposure to visible light, mycolactone A/B gave a mixture of four photomycolactones. We found that pentaenoates and tetraenoates, representing the unsaturated fatty acid portion of mycolactone A/B, show the reactivity profile parallel with that of mycolactone A/B. The structure of the four photomycolactones was elucidated via (1) structure determination of the four photoproducts in the tetraenoate series; (2) their transformation to the photoproducts in the pentaenoate and then mycolactone series. Triplet quenchers did not affect the photochemical transformation, thereby indicating an event at the singlet state. A concerted, photochemically allowed [ $4\pi s + 2\pi a$ ] cycloaddition was suggested to account for the observed result. This study provided the structurally defined and homogeneous material, which allowed demonstrating that photomycolactones exhibit significantly reduced cytotoxicity, compared with mycolactone A/B.

## ASSOCIATED CONTENT

### Supporting Information

Experimental procedures, characterization data, copies of spectra, and crystallographic data (CIF). This material is available free of charge via the Internet at <http://pubs.acs.org>.

## AUTHOR INFORMATION

### Corresponding Author

kishi@chemistry.harvard.edu

### Author Contributions

<sup>†</sup>These authors contributed equally to the work.

### Notes

The authors declare no competing financial interest.

## ACKNOWLEDGMENTS

Financial support from the Eisai USA Foundation is gratefully acknowledged. We thank Dr. Shao-Liang Zheng, Department of Chemistry and Chemical Biology, Harvard University, for the X-ray data collection and structure determination, and Drs. G. Lai and Nancy Wong, Eisai Inc., Andover, MA, for the MS/MS measurements.

## REFERENCES

- (1) For general reviews on Buruli ulcer and mycolactones, see: (a) Portaels, F.; Johnson, P.; Meyers, W., Eds. *Buruli Ulcer: Mycobacterium ulcerans infection*; World Health Organization: Geneva, Switzerland, 2001. (b) Hong, H.; Demangel, C.; Pidot, S. J.; Leadlay, P. F.; Stinear, T. *Nat. Prod. Rep.* **2008**, *25*, 447. (c) Kishi, Y. *Proc. Natl. Acad. Sci. U.S.A.* **2011**, *108*, 6703.
- (2) For example, see a review: Converse, P. J.; Nuernberger, E. L.; Almeida, D. V.; Grosset, J. H. *Future Microbiol.* **2011**, *6*, 1185.
- (3) George, K. M.; Chatterjee, D.; Gunawardana, G.; Welty, D.; Hayman, J.; Lee, R.; Small, P. L. *C. Science* **1999**, *283*, 854.
- (4) George, K. M.; Pascopella, L.; Welty, D. M.; Small, P. L. *C. Infect. Immun.* **2000**, *68*, 877.
- (5) Gunawardana, G.; Chatterjee, D.; George, K. M.; Brennan, P.; Whittren, D.; Small, P. L. *C. J. Am. Chem. Soc.* **1999**, *121*, 6092.
- (6) (a) Benewoitz, A. B.; Fidanze, S.; Small, P. L. C.; Kishi, Y. *J. Am. Chem. Soc.* **2001**, *123*, 5128. (b) Fidanze, S.; Song, F.; Szlosek-Pinaud, M.; Small, P. L. C.; Kishi, Y. *J. Am. Chem. Soc.* **2001**, *123*, 10117.
- (7) (a) Song, F.; Fidanze, S.; Benowitz, A. B.; Kishi, Y. *Org. Lett.* **2002**, *4*, 647; *Tetrahedron* **2007**, *63*, 5739. (b) Jackson, K. L.; Li, W.; Chen, C.-L.; Kishi, Y. *Tetrahedron* **2010**, *66*, 2263.
- (8) For synthetic studies of mycolactone A/B from other groups, see: (a) Negishi group: Yin, N.; Wang, G.; Qian, M.; Negishi, E. *Angew. Chem., Int. Ed.* **2006**, *45*, 2916. (b) Wang, G.; Yin, N.; Negishi, E. *Chem.—Eur. J.* **2011**, *17*, 4118. (c) Altmann group: Feyen, F.; Jantsch, A.; Altmann, K.-H. *Synlett* **2007**, 415. (d) Gersbach, P.; Jantsch, A.; Feyen, F.; Scherr, N.; Dangy, J.-P.; Pluschke, G.; Altmann, K.-H. *Chem.—Eur. J.* **2011**, *17*, 13017. (e) Chany, A.-C.; Casarotto, V.; Schmitt, M.; Tarnus, C.; Guenin-Mace, L.; Demangel, C.; Mirguez, O.; Eustache, J.; Blanchard, N. *Chem.—Eur. J.* **2011**, *17*, 14413. (f) Burkart group: Alexander, M. D.; Fontaine, S. D.; La Clair, J. J.; DiPasquale, A. G.; Rheingold, A. L.; Burkart, M. D. *Chem. Commun.* **2006**, 4602. (g) Feringa group: van Summeren, R. P.; Feringa, B. L.; Minnaard, A. J. *Org. Biomol. Chem.* **2005**, *3*, 2524.
- (9) The first e-mail exchange took place on May 5–7, 2011. We ran the photochemistry of mycolactone A/B in acetone on May 17, 2011, and isolated a mixture of the photomycolactones, which was sent to Professor Britton on May 25, 2011, for the biological tests.
- (10) For example, see: (a) Huber, T. W.; Reddick, R. A.; Kubica, G. P. *Appl. Microbiol.* **1970**, *19*, 383. (b) Even-Paz, Z.; Haas, H.; Sacks, T.; Rosenmann, E. *Br. J. Dermatol.* **1976**, *94*, 435. (c) Cope, R. B.; Hartman, J. A.; Morrow, C. K.; Haschek, W. M.; Small, P. L. C. *Photodermatol. Photoimmunol. Photomed.* **2002**, *18*, 271.
- (11) For example, see: Woodward, R. B.; Hoffmann, R. W. In *The Conservation of Orbital Symmetry*; VCH: Weinheim, 1970; pp 79–81.
- (12) For suprasterol-II, for example see: (a) Dauben, W. G.; Bell, I.; Hutton, T. W.; Laws, G. F.; Rheiner, A., Jr.; Urscheler, H. *J. Am. Chem. Soc.* **1958**, *80*, 4116. (b) Saunderson, C. P. *Acta Crystallogr.* **1965**, *19*, 187.
- (13) Ireland, C.; Scheuer, P. J. *Science* **1979**, *205*, 922.

- (14) Ireland, C.; Faulkner, J. *Tetrahedron* **1981**, *37*, 233.
- (15) For experimental details, see Supporting Information.
- (16) We referred to the major- and minor-product groups as A- and B-subgroups, unrelated to mycolactones A and B.
- (17) In the universal NMR database study, we introduced this term to describe a diastereomer due to stereogenic centers present outside a self-contained box. For example, see: (a) Kobayashi, Y.; Tan, C.-H.; Kishi, Y. *Helv. Chim. Acta* **2000**, *83*, 2562. (b) Higashibayashi, S.; Czechtizky, W.; Kobayashi, Y.; Kishi, Y. *J. Am. Chem. Soc.* **2003**, *125*, 14379.
- (18) For the  $^{13}\text{C}$   $\Delta\delta$  profile, see Supporting Information.
- (19) (a) Miller, A. K.; Trauner, D. *Angew. Chem., Int. Ed.* **2003**, *42*, 549. (b) Miller, A. K.; Trauner, D. *Synlett* **2006**, 2295 and references cited therein.
- (20) The absorption of *E,E,E,E*-isomer in methanol was  $\lambda_{\text{max}}$  330 nm ( $\log \epsilon$  4.87). For the absorption spectra of other geometrical isomers, see Supporting Information.
- (21) The ratio was estimated from the peak-intensity of  $^1\text{H}$  NMR spectrum and HPLC chromatogram. For details, see Supporting Information.
- (22) For an example related to this case in a broad sense, see: Budt, K.-H.; Vatele, J.-M.; Kishi, Y. *J. Am. Chem. Soc.* **1986**, *108*, 6080. We tested (*S*)-1,2-dimethoxypropane but found no significant effect on the ratio of remote diastereomers.
- (23) The observed acceleration appeared to reach the plateau at around 35°, which is interestingly close to the body temperature of humans, the host of *M. ulcerans* infection.
- (24) For example, see: (a) Turro, N. J. Page 257 In *Modern Molecular Photochemistry*; University Science Books: Sausalito, CA, 1991. (b) Griesbeck, A. G.; Mattay, J. *Synthetic Organic Photochemistry*; Marcel Dekker: New York, 2005; p 1.
- (25) (a) Bruückner, S.; Baldwin, J. E.; Moses, J.; Adlington, R. M.; Cowley, A. R. *Tetrahedron Lett.* **2003**, *44*, 7471. (b) Moses, J. E.; Baldwin, J. E.; Marquez, R.; Adlington, R. M.; Claridge, T. D. W.; Odell, B. *Org. Lett.* **2003**, *5*, 661.
- (26) For example, see: Hong, H.; Coutanceau, E.; Leclerc, M.; Caleechurn, L.; Leadlay, P. F.; Demangel, C. *PLoS Neglected Trop. Dis.* **2008**, *2*, e325.
- (27) The HPLC detection limit of mycolactone A/B was ~5 ng per injection (UV detector), whereas that of photomycolactones was ~250 ng (Waters 2424 ELS detector).
- (28) For example, **10-A1** gave the following growth inhibition against five cell lines: L929 ( $\text{GI}_{50}$  = 2020 nM (**10-A1**) vs 13 nM (**1**)), Hek-293 (2510 vs 3.3), Sk-Mel-5 (3600 vs 12), Sk-Mel-28 (470 vs 4.5), and A549 (3820 vs 4.7). Hande, S. M.; Xing, Y.; Burgett, A.; Shair, M. D.; Kishi, Y. Details of this study shall be reported elsewhere.
- (29) Marion, E.; Prado, S.; Cano, C.; Babonneau, J.; Ghamrawi, S.; Marsollier, L. *PLoS ONE* **2012**, *7*, e33600.

## EDITOR'S NOTE

Added at revision: By a total synthesis, we have recently established that the major and minor remote diastereomers in the B-series indeed correspond to **4-B2** and **4-B1**, respectively: Li, X.; Kishi, Y. 2012, unpublished work.